ULTRASONIC IMAGING **24,** 135- 146 (2002)

Doppler Angle Estimation of Pulsatile Flows Using AR Modeling

CHIH-KUANG YEH AND PAI-CHI LI

Department of Electrical Engineering
National Taiwan University
Taipei, Taiwan, R.O.C.
paichi@cc.ee.ntu.edu.tw

In quantitative ultrasonic flow measurements, the beam-to-flow angle (i.e., Doppler angle) is an important parameter. An autoregressive (AR) spectral analysis technique in combination with the Doppler spectrum broadening effect was previously proposed to estimate the Doppler angle. Since only a limited number of flow samples are used, real-time two-dimensional Doppler angle estimation is possible. The method was validated for laminar flows with constant velocities. In clinical applications, the flow pulsation needs to be considered. For pulsatile flows, the flow velocity is time-varying and the accuracy of Doppler angle estimation may be affected. In this paper, the AR method using only a limited number of flow samples was applied to Doppler angle estimation of pulsatile flows. The flow samples were properly selected to derive the AR coefficients and then more samples were extrapolated based on the AR model. The proposed method was verified by both simulations and *in vitro* experiments. A wide range of Doppler angles (from 30° to 78°) and different flow rates were considered. The experimental data for the Doppler angle showed that the AR method using eight flow samples had an average estimation error of 3.50° compared to an average error of 7.08° for the Fast Fourier Transform (FFT) method using 64 flow samples. Results indicated that the AR method not only provided accurate Doppler angle estimates, but also outperformed the conventional FFT method in pulsatile flows. This is because the short data acquisition time is less affected by the temporal velocity changes. It is concluded that real-time two-dimensional estimation of the Doppler angle is possible using the AR method in the presence of pulsatile flows. In addition, Doppler angle estimation with turbulent flows is also discussed. Results show that both the AR and FFT methods are not adequate due to the spectral broadening effects from the turbulence.

KEY WORDS: Autoregressive model; Doppler angle estimation; Doppler bandwidth; pulsatile flow; turbulent flow.

I. INTRODUCTION

Ultrasonic Doppler flow imaging has become a powerful tool in clinical applications. The Doppler effect, resulting from interaction of the ultrasonic wave with moving red blood cells, has been extensively used to determine blood flow velocity. However, conventional Doppler techniques can only estimate the axial component along the acoustic propagation direction. The projection of the velocity vector onto the transverse direction does not produce any Doppler shift. Thus, knowledge of the Doppler angle between the beam and flow directions is required in order to obtain the true flow velocity and to perform quantitative flow analysis.

To obtain two- or three-dimensional flow information, a number of approaches have been proposed.[1-5] One approach is the speckle tracking method. The two-dimensional velocity vector can be found by tracking the speckle pattern from consecutive B-mode images.[1,2] Another approach is to use a three-transducer set-up to measure the three-dimensional flow vector.[3] Since the transverse movement of the blood scatterers results in a modulation of the received signal, a modified autocorrelation approach that automatically compensates for the axial velocity when determining the transverse velocity was also proposed.[4] A similar approach has been suggested by Anderson based on spatial quadrature.[5]

0161-7346/02 $18.00

The Doppler spectrum broadening effect was also used to find the Doppler angle. Newhouse et al established the transverse Doppler theory describing the relationship between the Doppler angle and the bandwidth of the Doppler spectrum.[6, 7] The received bandwidth of the Doppler spectrum broadens as the scatterers travel through the focused ultrasound beam within a certain period of time. Tortoli et al demonstrated that the maximum frequency of the measured Doppler spectrum equals the Doppler shift frequency plus one half of the spectrum bandwidth even in the presence of velocity gradient.[8, 9] The maximum frequency of the Doppler spectrum can be related to the maximum velocity in the range cell that depends on the beam-to-flow angle. Based on the classic and transverse Doppler effects, Lee et al proposed a Doppler angle and flow velocity estimation method for both constant and pulsatile flow measurements.[10]

Based on the transverse Doppler theory, accurate Doppler spectral estimation is necessary to correctly calculate the Doppler angle. Fast Fourier Transform (FFT) based spectral estimators are typically used to obtain the Doppler spectrum. One problem with the FFT method is that a sufficiently long data acquisition time is required to achieve adequate spectral resolution. Therefore, the FFT method has only been applied to spectral Doppler modes and it is not suitable for real-time two-dimensional Doppler imaging.

To overcome the problem, a correlation-based method for Doppler angle estimation was proposed.[11] Variance of the Doppler spectrum is used to approximate the square of the Doppler bandwidth . In a color Doppler system, variance of the Doppler power spectrum is routinely calculated using a limited number of samples (e.g., 4-12). However, the method is limited in clinical applications due to the need of temporal and spatial averaging. On the other hand, an autoregressive (AR) spectral analysis technique using a limited number of flow samples (e.g., 8) was proposed.[12] The method does not require averaging and is able to accurately estimate the Doppler bandwidth. It also outperforms the conventional FFT method at small Doppler angles due to the ability to effectively increase the observation time by extrapolation. Since only a limited number of flow samples are used, real-time two-dimensional Doppler angle estimation is possible. The method has been validated for laminar flows with constant velocities.

In clinical applications, flow pulsation and turbulence need to be considered. In this case, the flow velocity is time-varying and the Doppler bandwidth is affected by the temporal velocity change within the data acquisition window. The AR method proposed by Yeh and Li is expected to outperform the conventional FFT method since the shorter data acquisition time required by the AR method is less affected by the temporal velocity change.[12] Therefore, it is the primary purpose of this paper to test this hypothesis. Doppler angle estimation using the AR method will be validated using both simulations and *in vitro* experiments. It will also be compared to the conventional FFT-based method. T he paper is organized as follows. In section II, the relations between the Doppler bandwidth and Doppler angle are reviewed. Principles of the proposed approach are also described. The performances of the angle estimator on simulated data are presented in section III and the experimental results are shown in section IV. The conclusions and discussion are described in section V.

II. MATERIALS AND METHODS

A. Basic principles of Doppler angle estimation

The Doppler frequency shift produced by the echoes backscattered from blood is used to measure the axial flow component of the flow velocity vector. The Doppler shift is related to the flow velocity by

$$f_d = \frac{2v}{\lambda}\cos\theta, \tag{1}$$

where f_d is the mean frequency of the Doppler spectrum, v is the flow velocity, λ is the acoustic wavelength and θ is the Doppler angle.

Because the Doppler bandwidth (B) is inversely proportional to the transit time of a scatterer crossing the acoustic sample volume,[8, 9] we have

$$B = \kappa \frac{v \cdot \sin\theta}{w}, \tag{2}$$

where κ is a scaling factor and w is the beam width. Therefore, given a Doppler spectrum and acoustic beam geometry, the Doppler angle θ can be found by

$$\theta = \tan^{-1}\left(\frac{w \cdot B}{\kappa \cdot v \cdot \cos\theta}\right). \tag{3}$$

Apparently, the accuracy of Doppler angle estimation is determined by the accuracy of the spectrum estimator from Eq. (3).

In practice, the Doppler spectrum is broadened due to spatial velocity variations (i.e., velocity gradient).[7, 8] To overcome this problem, Tortoli et al demonstrated that in the presence of a velocity gradient, the maximum Doppler frequency (f_{max}) still remains the same and can be represented as the Doppler frequency shift plus one half of the Doppler spectrum bandwidth.[9] Lee et al extended the relation to derive the Doppler angle formula as[10]

$$\theta = \tan^{-1}\left(\frac{f_{\max} - f_d}{f_d} \cdot \frac{2F}{W}\right), \tag{4}$$

where F is the transducer focal length and W is the transducer width. In this paper, Eq. (4) is used to estimate the Doppler angle.

B. Principles of autoregressive method

Traditionally, the Doppler spectrum is estimated using the FFT. In this paper, the AR method is used for Doppler spectral estimation. Based on the AR model, the current value of a Doppler signal $y(n)$ can be described by a linear combination of previous values of the same Doppler signal and a white noise input.[13] Note that the Doppler signal contains flow information at a particular range (or range gate). It is inherently discrete with a sampling interval equal to the pulse repetition interval (PRI). For a p-th order AR model, we have

$$y(n) = e(n) - a_1 y(n\text{-}1) - a_2 y(n\text{-}2) - \ldots - a_p y(n\text{-}p), \tag{5}$$

where $e(n)$ is a white, stochastic signal driving the AR process and the a_i's are the prediction coefficients of the p-th order AR-model. The variance of $e(n)$ and the coefficients a_i's can be estimated by solving the Yule-Walker equations. Once the parameters are computed, future values of the Doppler signal can be extrapolated. In other words, given the Doppler signal for $y(n-1)$ to $y(n-p)$, the Doppler signal for $y(n\text{-}p\text{+}1)$, ..., $y(n)$ can be extrapolated, assuming the coefficients a_i's are accurately estimated.

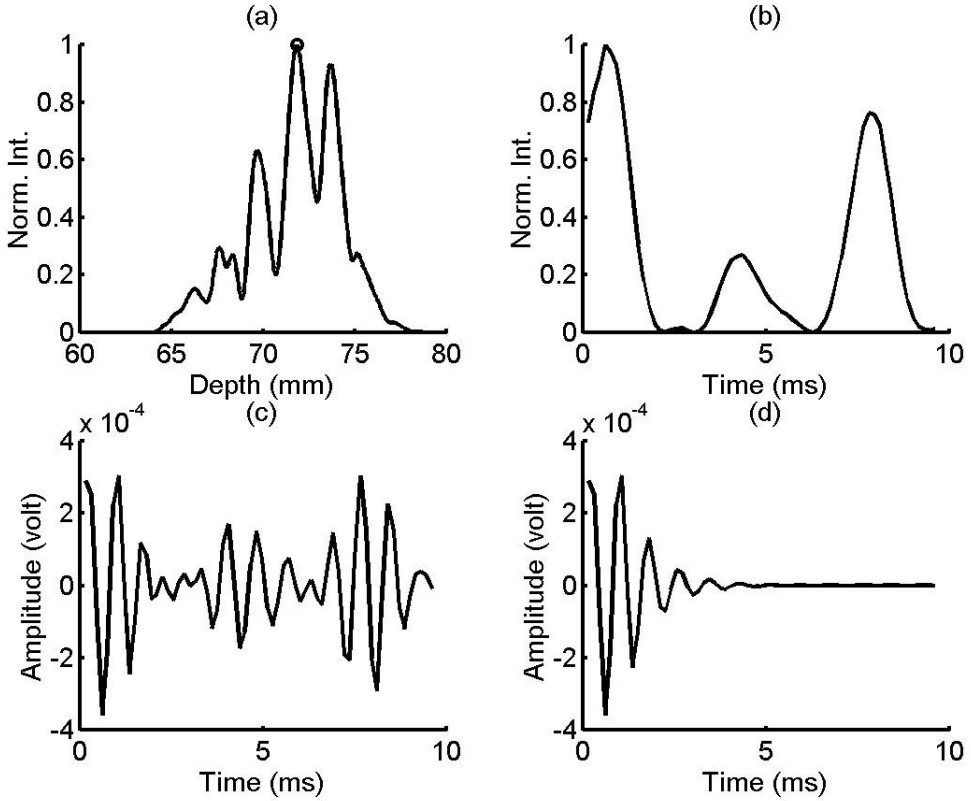

FIG. 1 Selection of the Doppler signal. (a) Signal intensity (depth direction). (b) Doppler signal intensity (Doppler temporal direction). (c) Original Doppler signal. (d) Extrapolated Doppler signal.

Three issues need to be addressed when implementing the AR model. The first issue is selection of the model order. If the order is too low, not all features of the signal are described. If the order is too high, on the other hand, false peaks and line splitting may be present.[13] This issue in the context of Doppler signal extrapolation will be further discussed in the following section.

The second issue is selection of the Doppler signal to be extrapolated. Our previous results have suggested that, assuming a p-th order AR model, the p flow samples can be used for Doppler angle estimation if the following two conditions are simultaneously satisfied.[12] First, one of the flow samples must contain the maximum in the depth (a.k.a. fast time) direction such that a local maximum signal-to-noise ratio is guaranteed. Second, signal intensity of the Doppler signal increases and reaches a peak before it starts to decrease along the Doppler temporal (a.k.a. slow time) direction. For a particular depth or within a certain range gate, the signal along the Doppler temporal direction is defined as the Doppler signal. The second criterion implies that the scatterers of interest cross the center of a beam during the observation time.

The criteria can be explained in figure1. In (a), the circle corresponds to a maximum along the depth direction. Panel (b) shows the Doppler signal intensity (i.e., square of the envelope) after baseband demodulation along the Doppler temporal direction at the depth defined in (a). In this case, a peak is found in the first few samples and, hence, the flow samples can be used. Panel (c) corresponds to the original radiofrequency (rf) Doppler signal. The extrapolated Doppler signal using the first eight samples are shown in (d). It has been shown

that the data selection process can effectively choose valid Doppler samples and reduce interference from multiple scatterers.[12]

The third issue of this approach relates to the sample volume. In our previous study, effects of the aspect ratio (i.e., the ratio of length of the Doppler range gate to the lateral beam width) of the sample volume with the AR method were discussed.[11, 12] For a large aspect ratio (e.g., 5), there was a good agreement between the AR method and the theoretical values at large Doppler angles and high velocities. At lower Doppler angles, there was a significant deviation between the predicted values and the theoretical values for aspect ratios smaller than 5. This is due to the fact that with a small aspect ratio, the path length along the flow direction quickly deviates from the assumed value as the Doppler angle decreases from 90^{o}.[9, 10] Effects of the velocity gradient on the AR-based Doppler angle estimation method were also investigated. The results show that the estimation error of the AR method increases with the degree of spatial velocity gradient and decreases with the aspect ratio. On the other hand, the AR method had an average estimation error of 3.6^{o} in the experimental data for Doppler angles ranging from 33^{o} to 72^{o}.[12] Based on our previous findings, the aspect ratio is set to 5 in this study.

III. RESULTS ON SIMULATED DATA

A. Pulsatile flows

Simulations of pulsatile flows were performed to test the proposed approach. The simulation model consisted of two parts. The first part included blood scattering and the acoustic point spread function. The response of each scatterer was calculated using an acoustic impulse response method.[14] The second part was for the time-varying velocity profile of pulsatile flows.[15, 16] The velocity at a particular point in the vessel changed with time due to flow acceleration and deceleration. In this study, the flow velocity profiles emulated flows in the carotid artery.

In the simulations, the transducer was a linear array with a center frequency of 3.5 MHz and a 19 mm aperture size. The sample volume was located at the focal point, which was 70 mm away from the transducer. The corresponding pulse-echo –6 dB beam width was about 1.4 mm at the focal point. The sound velocity was 1,540 m/s and the PRI was 150 μs. The heart rate was 80 per minute (i.e., the duration of a heart cycle was 0.75 s). Figures 2(a)-(d) represent the temporal velocity distributions during a single cardiac cycle with the mean velocities at 3, 9, 15, and 21 cm/s, respectively. The Doppler angle in this case was 45^{0}. Note that inverted brightness is displayed in figures 2 (a)-(d) (i.e., the signal intensity increases as the display brightness decreases).

Regarding the Doppler angle estimation, 64 samples were obtained by extrapolating eight original flow samples. The resultant 64 samples were then Fourier transformed to obtain the Doppler spectrum. This is also referred to as the AR method. The spectrum was also compared to the spectrum obtained by Fourier transforming 64 original flow samples. This is referred to as the FFT method. The order of the AR model was selected such that the prediction error (*PE*) was minimized. The prediction error is given by

$$PE = E\left\{(y(n) - y'(n|p))^2\right\}, \tag{6}$$

where $y(n)$ is the original data, and $y'(n|p)$ is an extrapolated data set based on a p-th order AR model.[12] By definition, *PE* was 100% with an order of 1. In the simulations, 64 samples starting from 0.1 second relative to the beginning of the heart cycle shown in figures 2 (a)-(d)

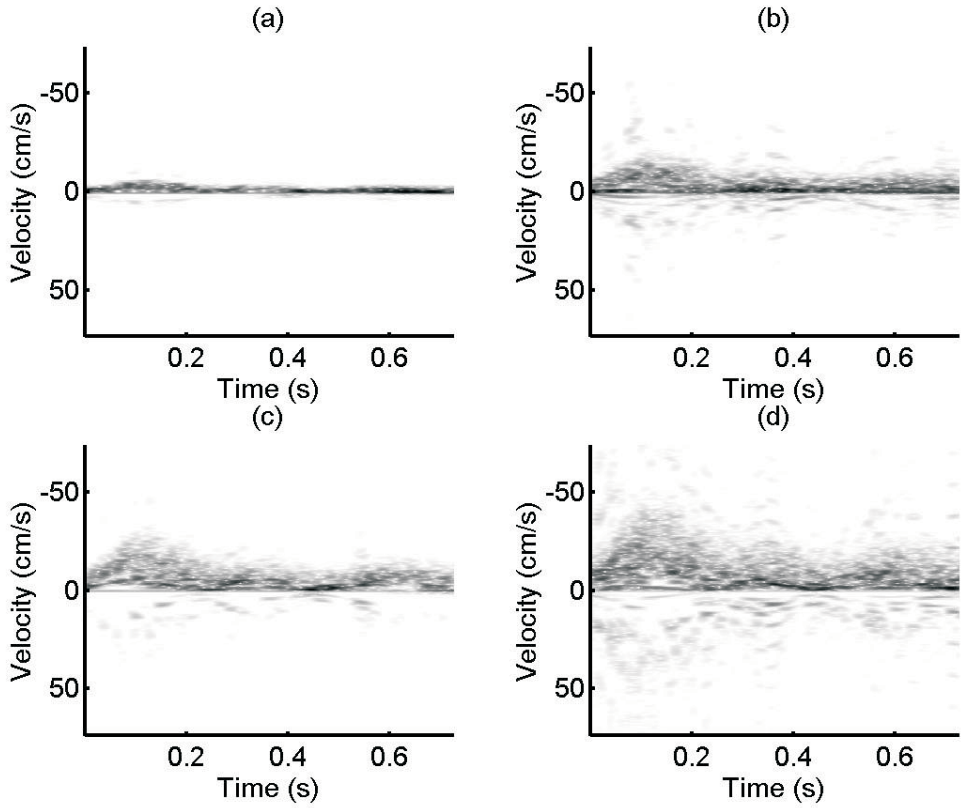

FIG. 2 Velocity distribution with mean velocities at (a) 3 cm/s, (b) 9 cm/s, (c) 15 cm/s and (d) 21 cm/s. The Doppler angle was 45°. Note that inverted brightness is displayed (i.e., the signal intensity increases as the display brightness decreases).

were selected. The four Doppler signals were then used to test the order selection criterion of the AR model. T he four prediction errors as a function of the model order are shown in figure 3. The solid, dash-dotted, dashed, and dotted lines represent the mean velocities of 3, 9, 15, and 21 cm/s, respectively. The four *PE* curves show that the prediction errors decrease as the order increases. 20% *PE* error was used as the threshold. Based on figure 3, the four *PE* curves at an order of 8 were all below 20%. Hence, an 8-th order AR model was used in the following simulations.

The results of Doppler angle estimation using the AR method and the FFT method are shown in figures 4 and 5, respectively. In each figure, (a)-(d) represent the results at mean velocities of 3, 9, 15, and 21 cm/s, respectively. Totally, fifteen Doppler angle estimates were obtained within the duration of a heart cycle. The actual Doppler angles (i.e., 45°) are shown as the horizontal dashed lines. The asterisks represent the estimated Doppler angles. The AR method had an average estimation error of 2.61° and a standard deviation of 3.19° (Fig. 4), whereas the FFT method had an average error of 5.41° and a standard deviation of 6.16° (Fig. 5).

Different Doppler angles were also considered in this study. The Doppler angle varied from 30° to 78°. Other ultrasonic parameters were the same as those used in previous simulations. The means and the standard deviations of the estimation errors were summarized in Table 1. Tables 1 (a) and (b) show the Doppler angle estimates using the AR method and the FFT method, respectively. The simulation data for the AR method had an average estimation

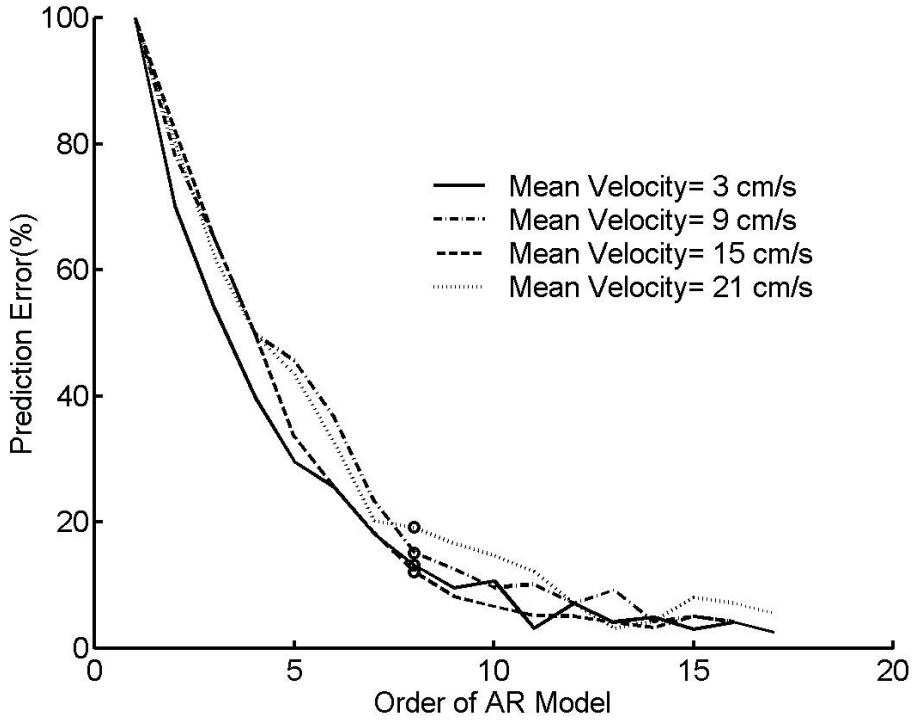

FIG. 3 Four prediction error curves in % vs. the AR model order.

TABLE 1. Summary of the errors of Doppler angle estimation using the (a) AR method and (b) FFT method with simulation data. All results are mean ± one standard deviation.

(a)

Doppler angle	Peak velocity (cm/s)			
(°)	10	30	50	70
30	2.42 ± 2.78	1.87 ± 2.24	2.00 ± 2.87	2.50 ± 3.14
45	2.71 ± 3.17	3.03 ± 3.56	2.35 ± 3.19	2.35 ± 2.83
55	2.44 ± 3.20	3.09 ± 3.56	1.87 ± 2.51	2.01 ± 2.38
65	2.58 ± 3.16	2.69 ± 3.83	2.78 ± 3.39	2.17 ± 2.53
78	2.93 ± 3.82	1.66 ± 1.88	2.30 ± 3.18	2.10 ± 2.58

(b)

Doppler angle	Peak velocity (cm/s)			
(°)	10	30	50	70
30	7.45 ± 5.56	6.54 ± 5.24	5.96 ± 4.58	6.58 ± 5.19
45	5.48 ± 5.85	5.54 ± 6.32	5.16 ± 5.80	5.47 ± 6.66
55	5.75 ± 8.54	6.81 ± 7.53	7.31 ± 8.54	6.34 ± 5.45
65	5.81 ± 6.45	5.84 ± 6.56	5.57 ± 6.82	5.15 ± 4.87
78	7.23 ± 4.87	6.63 ± 7.98	6.04 ± 5.68	4.78 ± 5.91

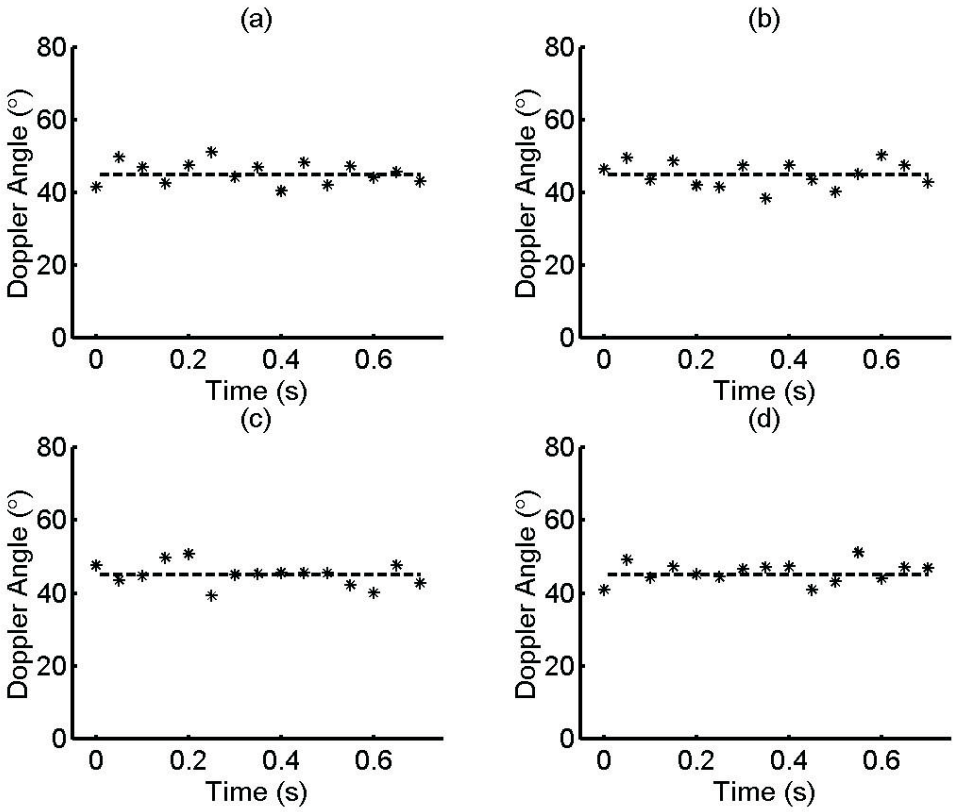

FIG. 4 Simulation results of the estimated Doppler angles using the AR model with the mean velocities at (a) 3 cm/s, (b) 9 cm/s, (c) 15 cm/s and (d) 21 cm/s. The Doppler angle was 45^0.

error of 2.39^o and an average error of 6.07^o for the FFT method. The results indicate that the AR method provides more accurate Doppler angle estimates than the FFT method. This is because that the AR method only uses eight Doppler signals, whereas the FFT method uses 64 Doppler signals. Hence, the AR method is less affected by the temporal velocity change.

B. Turbulent flows

Turbulent flows may be present in clinical applications of Doppler angle estimation. In the cardiovascular system, for example, turbulence has been associated with poststenotic dilatation, aneurysms, atherogenesis and thrombosis.[18,19] With turbulent flows, significant velocity variations exist within the sample volume. In this case, the Doppler angle estimation using the AR or FFT method is similarly affected by the spatial flow velocity changes. The Doppler angle estimation in turbulent flows using the AR and FFT methods was investigated using simulations. The turbulence was modeled as an irregular motion occurring about the mean velocity and random velocity components were used to generate the Doppler signal.[19] In the simulations, the Doppler signal in the presence of turbulence was simulated by having the scatterers move with a two-dimensional random velocity. The magnitude of the velocity was uniformly distributed within ± 50% around a mean velocity that corresponded to the velocity of a constant flow. The direction of the velocity also varied between ± 50% around the primary Doppler angle.

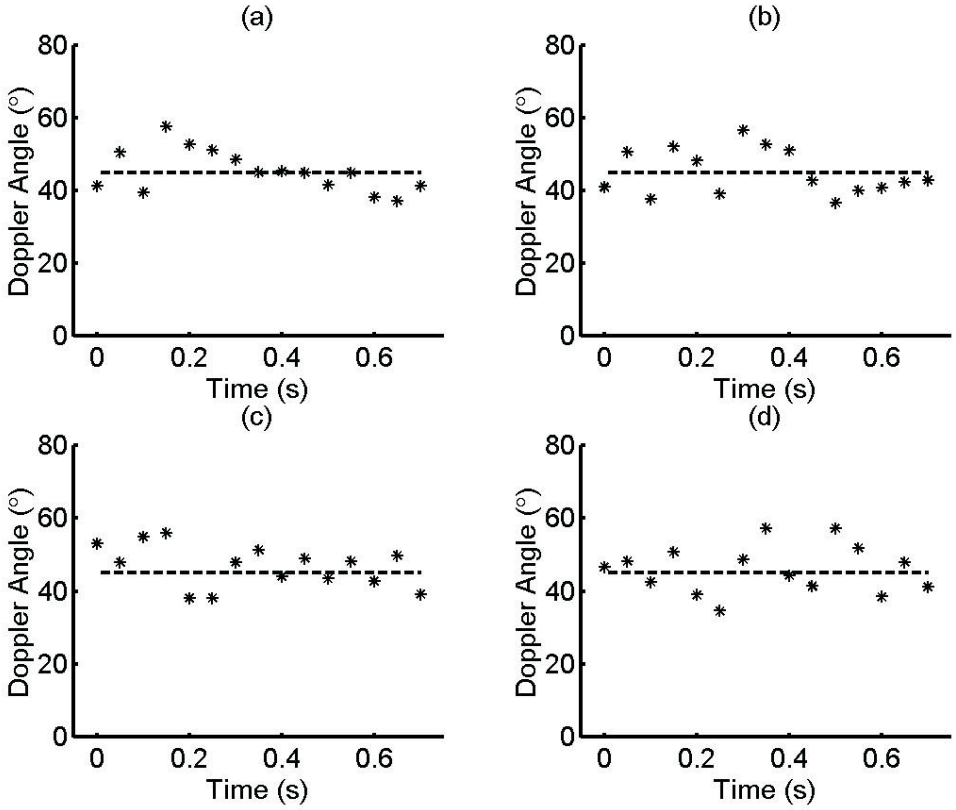

FIG. 5 Simulation results of the estimated Doppler angles using the conventional FFT method with mean velocities at (a) 3 cm/s, (b) 9 cm/s, (c) 15 cm/s and (d) 21 cm/s. The Doppler angle was 45^{0}.

The simulation model and related parameters were the same as that described previously. Sixty four Doppler signals were simulated for each case. The laminar flows with constant velocities were introduced to compare with flows with turbulence. The maximum velocity was 30 cm/s. Figures 6 (a)-(d) represent the distributions of Doppler spectrum using FFT with Doppler angles of 30^{o}, 45^{o}, 60^{o}, and 75^{o}, respectively. The solid and dotted lines represent the results of laminar flows with constant velocities and turbulent flows, respectively. The results show that the Doppler bandwidth of a turbulent flow is broader than that of a laminar flow with constant velocity.

The Doppler angle estimates in turbulent flows with five Doppler data sets at each angle are shown in figure 7. Figure 7(a) shows the estimated Doppler angles using the AR method, which had an average estimation error of 17.3^{o}. The FFT method using 64 flow samples had an average error of 15.7^{o} as shown in figure 7(b). The results show that both the AR and FFT methods are not suitable to estimate Doppler angles when the Doppler spectrum is affected by turbulence.

IV. RESULTS ON EXPERIMENTAL DATA

Experiments were also conducted to investigate the performance of the AR method. A block diagram of the experimental system is shown in figure 8. The pulsatile flow was generated by the CompuFlow1000 flow system (Shelley Medical Imaging Technologies, On-

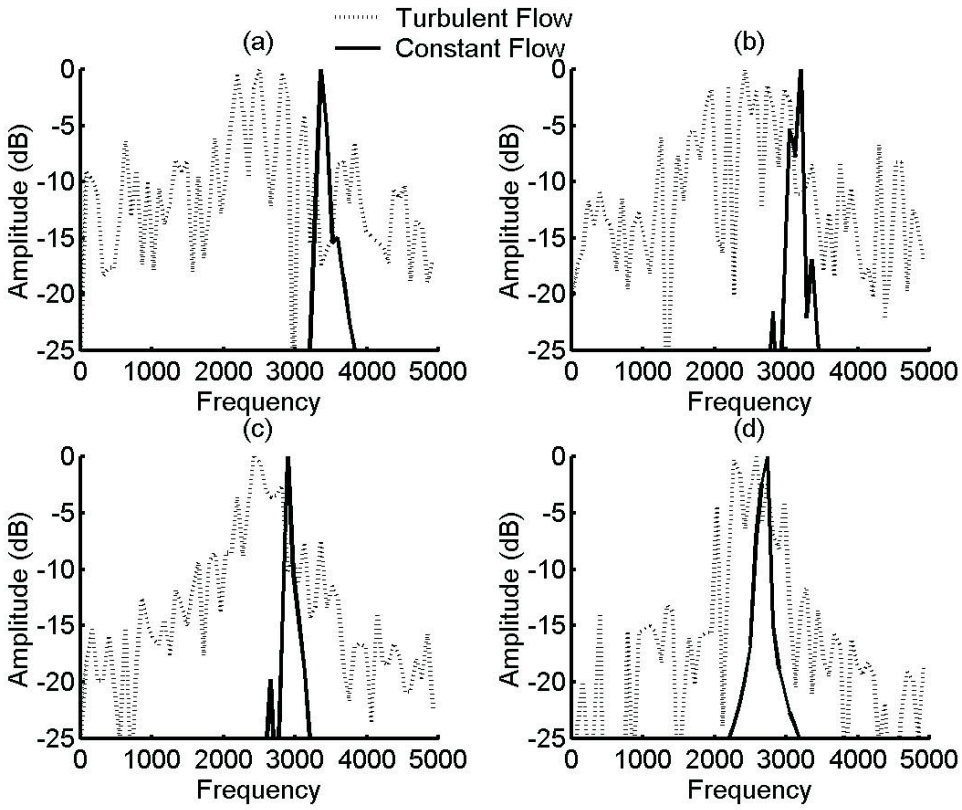

FIG. 6 The Doppler spectra of laminar flow with constant velocity (solid) and flow with turbulence (dotted). The Doppler angles are (a) 30^0, (b) 45^0, (c) 60^0 and (d) 75^0.

tario, Canada). A blood-mimicking fluid (Shelley Medical Imaging Technologies, Ontario, Canada) was used as the scattering source. The heart cycle was 0.752 s. A silicone tube with an 8 mm internal diameter was used as the vessel.

The data acquisition system consisted of a pulser/receiver (Panametrics 5072, MA, USA) with a 12-bit, 80 Msamples/s arbitrary function generator (CompuGen 1100, Gage, Montreal, Canada) and a 12-bit, 100 Msamples/s A/D converter (CompuScope 12100, Montreal, Canada). The sampling frequency of the A/D converter was 20 Msamples/s. The arbitrary function generator was used to externally trigger the pulser with a PRI of 150 μs. The equipment was controlled by a personal computer under LabVIEW (National Instruments, TX, USA). After the returning echoes were amplified, the signals were then sampled by the A/D converter and stored for off-line signal processing. Data analysis and graphic display were done on a personal computer using MATLAB (MathWorks Inc., MA, USA). The transducer (Panametrics V381, MA, USA) had a center frequency of 3.5 MHz and a fixed focus at 70 mm. The diameter of the transducer was 19 mm making the two-way –6 dB beam width about 1.4 mm at the focal point. In this study, two D/A converters were used to ensure that the CompuFlow1000 flow system and the data acquisition system were synchronized.

In the experiments, four arterial flows with peak velocities at 10, 30, 50, and 70 cm/s were used. The four flows corresponded to mean velocities (i.e., temporal averages) at 3, 9, 15, and 21 cm/s, respectively. The velocity profile with the peak velocity at 10 cm/s (defined by the CompuFlow 1000 flow system) is shown in figure 9(a). The Doppler angle was 45^0. Note that the Doppler signal from 0 to 0.285 s (denoted by the dashed line in figure 9(a)) in

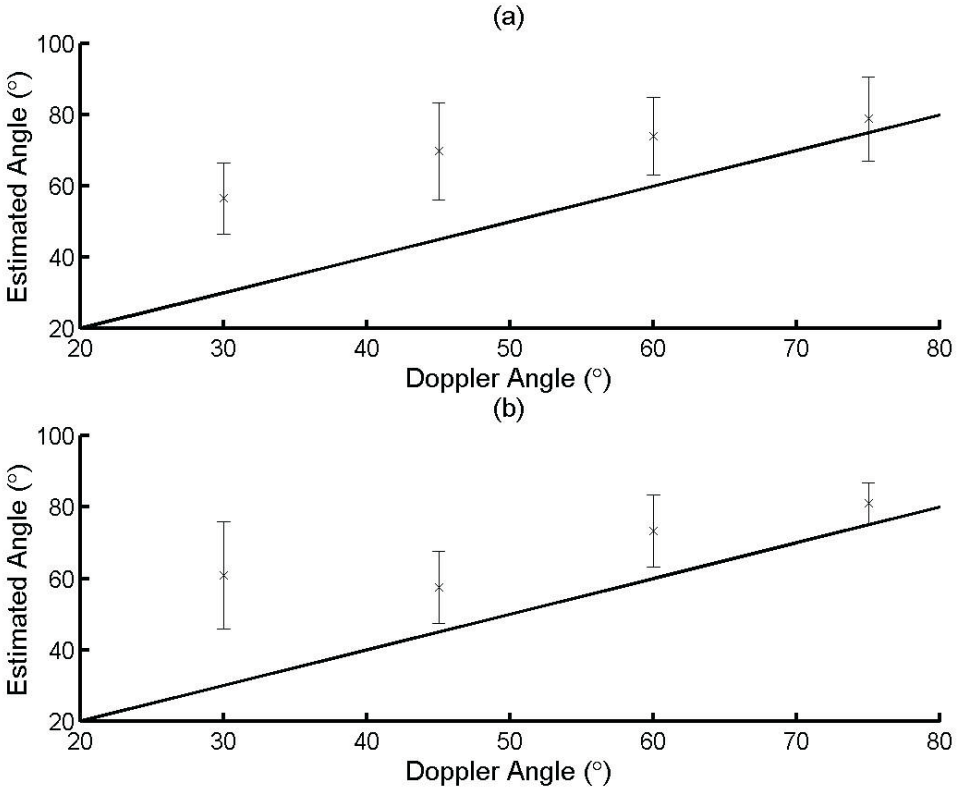

FIG. 7 Doppler angles estimated for simulated data of turbulent flows using (a) the AR method and (b) the FFT method. The solid lines are the true angles. The error bars represent ± one standard deviation relative to the mean value ('× ').

the arterial flow was collected. The portion of the Doppler signal also included the peak velocity, where the velocity variation was the greatest. Figure 9(b) shows the corresponding grayscale M-mode image of the Doppler signal collected by the experimental system with a dynamic range of 40 dB. The two horizontal dashed white lines represent the upper and the bottom vessel walls, respectively.

The Doppler angles used in the experiments were 30°, 45°, 55°, 65° and 78°. At each angle, five data sets were used. For each data set, Doppler angles were estimated every 0.05 s. In addition, the data selection criteria described in section II were applied. In other words, one of the flow samples must contain the maximum in the axial direction and the signal intensity of the Doppler signal increases and reaches a peak before it starts to decrease along the Doppler temporal direction. Results of the Doppler angle at 45° using the AR method and the FFT method are shown in figures 10 and 11, respectively. Panels (a)-(d) represent the flows with peak velocities of 10, 30, 50 and 70 cm/s, respectively. The dashed lines in all panels are the true Doppler angle. In figure 10, the AR method had an average estimation error of 3.75° (average estimate denoted by 'x') and the standard deviation ranged from 3.71° to 4.31° (denoted by the error bar). The results from the FFT method using 64 original flow samples as shown in figure 11 had an average error of 6.87° and the standard deviation ranged from 6.03° to 8.00°.

The mean values and standard deviations of Doppler angle estimation with different Doppler angles (from 30° to 78°) and flow rates were summarized in table 2. Other ultrasonic parameters were the same as those used in previous experiments. Tables 2 (a) and (b) show

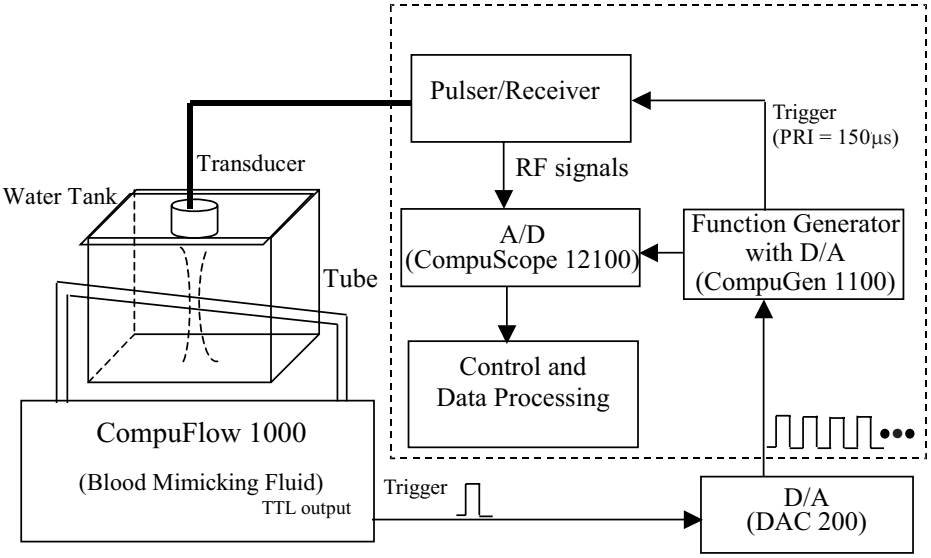

FIG. 8 Experimental system set-up.

TABLE 2. Summary of the errors of Doppler angle estimation using the (a) AR method and (b) FFT method with experimental data. All results are mean ± one standard deviation.

(a)

Doppler angle	Peak velocity (cm/s)			
(°)	10	30	50	70
30	2.93 ± 3.33	3.05 ± 3.06	3.30 ± 2.74	3.77 ± 3.19
45	3.46 ± 3.71	3.95 ± 4.31	4.05 ± 4.04	3.53 ± 3.99
55	3.77 ± 3.54	3.43 ± 3.62	3.42 ± 3.69	3.99 ± 3.14
65	2.75 ± 3.45	3.51 ± 3.32	3.96 ± 3.38	4.65 ± 4.01
78	3.40 ± 3.38	2.54 ± 2.88	3.06 ± 3.13	4.13 ± 3.02

(b)

Doppler angle	Peak velocity (cm/s)			
(°)	10	30	50	70
30	8.87 ± 7.51	7.24 ± 5.96	8.62 ± 5.02	6.46 ± 7.19
45	6.45 ± 6.70	6.50 ± 6.03	7.33 ± 8.00	7.20 ± 6.19
55	6.98 ± 6.26	5.41 ± 6.57	6.58 ± 7.02	8.34 ± 7.41
65	5.51 ± 7.24	6.38 ± 5.56	8.05 ± 6.25	7.95 ± 6.87
78	6.94 ± 5.67	5.54 ± 6.52	7.54 ± 5.18	7.81 ± 6.13

the Doppler angle estimates using the AR method and FFT method, respectively. The experimental data for the AR method had an average estimation error of 3.50° and an average error of 7.08° for the FFT method. The experimental results also indicate that AR method outperformed the FFT method.

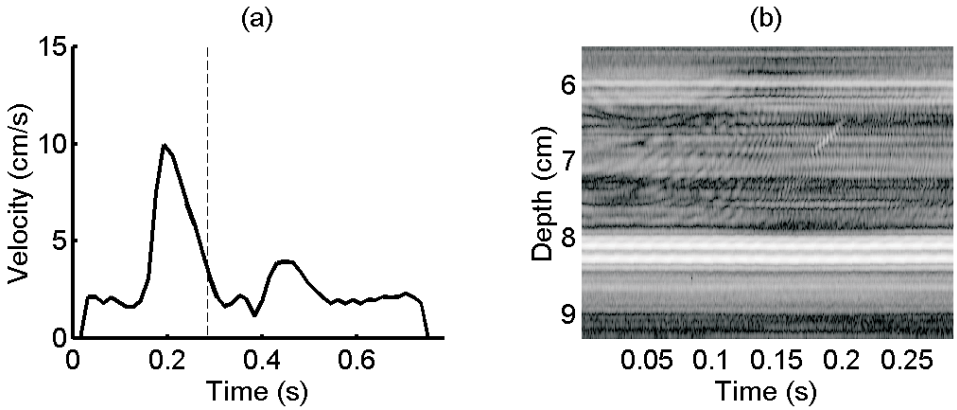

FIG. 9 Experimental data for a pulsatile flow with the peak velocity at 10 cm/s. (a) Velocity profile of the arterial flow. (b) M-mode image.

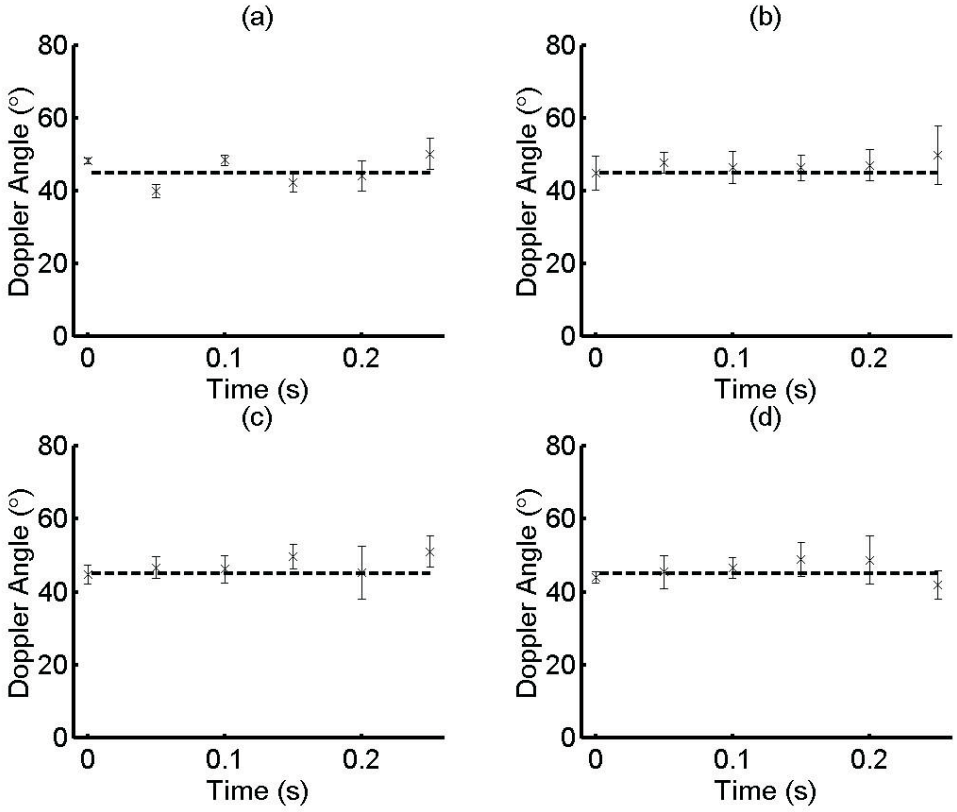

FIG. 10 Estimated Doppler angles using the AR method. The real angle is 45°. Peak velocities are (a) 10 cm/s, (b) 30 cm/s, (c) 50 cm/s and (d) 70 cm/s. Error bars represent ± one standard deviation relative to the mean value.

The relative performance of the AR and FFT method depends on the signal-to-noise ratio (SNR).[17] The SNR is defined as the ratio of the average signal power to the average noise power. Marasek and Nowicki compared the performance of various spectral estimation techniques for maximum frequency estimation of the Doppler spectra.[17] It was concluded that the performance of the spectral estimation techniques depended on the SNRs and accu-

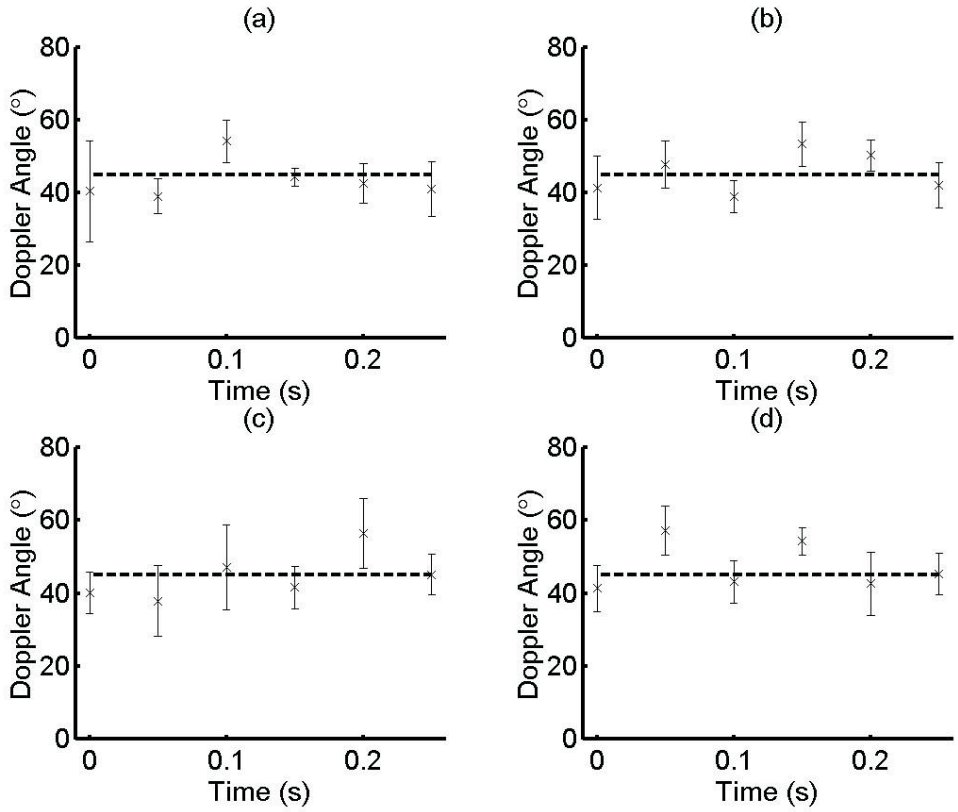

FIG. 11 Estimated Doppler angles using the FFT method. The real angle is 45°. Peak velocities are (a) 10 cm/s, (b) 30 cm/s, (c) 50 cm/s and (d) 70 cm/s. Error bars represent ± one standard deviation relative to the mean value.

rate estimation results can be obtained only for signals with SNR > 3dB. In our study, the SNRs were equal to 20 dB and 10.5 dB (> 3dB) for the simulations and experiments, respectively. Thus, the AR and the FFT method are both suitable to estimate the Doppler spectra.

V. CONCLUSIONS AND DISCUSSION

In this paper, an AR approach using a limited number of flow samples for Doppler angle estimation was applied to pulsatile flows. An 8-th order AR model was used to extrapolate the original 8 flow samples to 64 flow samples for spectral estimation. Based on simulation and experimental results, the AR method not only accurately estimated the Doppler angle, but also outperformed the conventional FFT method. The main reason for this is that the data acquisition time required by the AR method is smaller and hence it is less affected by the temporal velocity change.

In the presence of the turbulent flows, however, the AR method is not suitable for estimating the Doppler angle due to the fact that the Doppler bandwidth is not only affected by the transit time effect, but it is also affected by the turbulence. In this study, the experimental results had larger estimation errors than the simulation results. This is possibly due to the difference of the SNRs. In other words, the lower SNR associated with the experimental data potentially induced more extrapolation errors when the AR method was applied.

In a previous study, the performance of the AR method in the constant velocity flows was validated.[12] The spatial velocity gradient associated with a laminar flow had noticeable impact on the estimation results. Errors of the AR method increased with the gradient. In the previous study, the AR method had an average estimation error of 3.6° in the experimental data for the Doppler angle ranging from 33° to 72°.[12] For pulsatile flows, the Doppler bandwidth is affected by both the spatial and temporal velocity changes. The experimental data for the AR method in this study had an average estimation error of 3.5° for a Doppler angle range from 30° to 78°. It was found that the spatial velocity change (i.e., gradient) has a bigger impact on Doppler angle estimation than the temporal velocity change (i.e., pulsation) with the AR method. However, the FFT method is significantly affected by both the spatial and temporal velocity changes. For the FFT method, the average estimation errors for constant flows and for pulsatile flows were 4.7° and 6.87°, respectively.

Finally, the results shown in the paper indicate that real-time two-dimensional Doppler angle estimation using the AR method in the presence of pulsatile flows is feasible. Although the computational complexity associated with the AR method is more demanding than that with the conventional FFT method, such computational requirements can be adequately met and do not affect the two-dimensional imaging frame rate. [20]

ACKNOWLEDGMENTS

Support supplied by National Science Council under grant NSC 89-2213-E-002-128 is gratefully acknowledged. Comments from the anonymous reviewers are also greatly appreciated.

REFERENCES

1. Bohs, L. N., Friemel, B. H. and Trahey, G. E., Experimental velocity profiles and volumetric flow via two-dimensional speckle tracking, *Ultrasound Med. Biol. 21*, 885-898 (1995).

2. Bohs, L. N., Geiman B. J. Anderson M. E. et al., Ensemble tracking for 2D vector velocity measurement: experimental and initial clinical results, *IEEE Trans. Ultrason. Ferroelect. Freq. Contr. 45*, 912-924 (1998).

3. Hein, I., A., 3-D flow velocity vector estimation with a triple-beam lens transducer experimental results, *IEEE Trans. Ultrason. Ferroelect. Freq. Contr. 44*, 85-89 (1997).

4. Jensen, J.A., A new estimator for vector velocity estimation, *IEEE Trans. Ultrason. Ferroelect. Freq. Contr. 48*, 886-894 (2001).

5. Anderson, M.E., Multi-dimensional velocity estimation with ultrasound using spatial quadrature, *IEEE Trans. Ultrason. Ferroelect. Freq. Contr. 45*, 852-861 (1998).

6. Newhouse, V.L., Censor, D., Vontz, T. et al., Ultrasound Doppler probing of flow estimation using two transducers and spectral width, *IEEE Trans. Ultrason. Ferroelect. Freq. Contr. 41*, 90-95 (1994).

7. Newhouse, V.L., Censor, D., Vontz, T. et al., Ultrasound Doppler probing of flows transverse with respect to beam axis, *IEEE Trans. Biomed. Eng. 34*, 779-789 (1987).

8. Tortoli P., Guidi G., Mariotti V. and Newhouse, V.L., Experimental proof of Doppler bandwidth invariance, *IEEE Trans. Ultrason. Ferroelect. Freq. Contr. 39*, 196-203 (1992).

9. Tortoli P., Guidi G. and Newhouse V.L., Improved blood velocity estimation using the maximum Doppler frequency, *Ultrasound Med. Biol. 21*, 527-532 (1995).

10. Lee B.R., Chiang, H. K., Chou, Y.H., et al., Implementation of spectral width Doppler in pulsatile flow measurements, *Ultrasound Med. Biol. 25*, 1221-1227 (1999).

11. Li, P.C., Cheng, C.J. and Shen, C.C., Doppler angle estimation using correlation. *IEEE Trans. Ultrason. Ferroelect. Freq. Contr. 47,* 188-196 (2000).

12. Yeh, C.K. and Li, P.C., Doppler angle estimation using AR modeling, *IEEE Trans. Ultrason. Ferroelect. Freq. Contr. 49,* 683-692 (2002).

13. Kay, S.M., *Modern spectral estimation: Theory and application* (Englewood Cliffs, NJ: Prentice Hall, 1988).

14. Kerr, A.T. and Hunt, J W., A method for computer simulation of ultrasound Doppler color flow images-I. Theory and numerical method, *Ultrasound Med. Biol. 18*, 861-872 (1992).

15. Evans, D.H., Some aspects of the relationship between instantaneous volumetric blood flow and continuous wave Doppler ultrasound recordings III, *Ultrasound Med. Biol. 9*, 617-623 (1982).

16. Jensen, J.A. *Estimation of blood velocity using ultrasound: A signal processing approach* (New York: Cambridge University Press, 1996).

17. Marasek, K. and Nowicki, A., Comparison of the performance of 3 maximum Doppler frequency estimators coupled with different spectral estimation methods, *Ultrasound Med. Biol. 20,* 629-638 (1994).

18. Bascom, P. A. J., Cobbold, R. S. C., Routh, H. F. et al., On the Doppler signal from a steady flow asymmetrical stenosis model: effects of turbulence, *Ultrasound Med. Biol. 19,* 197-210 (1993).

19. Cloutier, G., Chen, D. and Durand L.-G., Performance of time-frequency representation techniques to measure blood flow turbulence with pulsed-wave Doppler ultrasound. *Ultrasound Med. Biol. 27,* 535-550 (2001).

20. Schlindwein, F. S. and Evans, D. H., A real-time autoregressive spectrum analyzer for Doppler ultrasound signals, *Ultrasound Med. Biol. 15,* 263–272 (1989).